Synthesis of Chiral Cationic (Diimino- and diaminodiphosphane)ruthenium Complexes and Their Applications in Catalytic Oxidation − Crystal Structures of *cis*-[RuCl(py){κ^4-$Ph_2PC_6H_4CH{=}NC_6H_{10}N{=}CHC_6H_4PPh_2$}]$BF_4$ and *cis*-[RuCl(py){κ^4-$Ph_2PC_6H_4CH{=}NC_6H_{10}N(H)CH_2C_6H_4PPh_2$}]$BF_4$

Wai-Kwok Wong,*[a] Xiao-Ping Chen,[a] Tat-Wai Chik,[a] Wai-Yeung Wong,[a] Jian-Ping Guo,[a] and Fu-Wa Lee[a]

Keywords: Catalysis / Chiral complexes / Oxidation / N,P ligands / Ruthenium

Halide abstraction of *trans*-[$RuCl_2${κ^4-(1*R*,2*R*)-PNNP}] {(1*R*,2*R*)-PNNP = (1*R*,2*R*)-*N*,*N*′-bis[2-(diphenylphosphanyl)-benzylidene]-1,2-diiminocyclohexane} and *trans*-[$RuCl_2${κ^4-(1*R*,2*R*)-P(NH)(NH)P}] {(1*R*,2*R*)-P(NH)(NH)P = (1*R*,2*R*)-*N*,*N*′-bis[2-(diphenylphosphanyl)benzylidene]-1,2-diaminocyclohexane} with $AgBF_4$ in acetonitrile at ambient temperature gave *cis*-[RuCl(CH_3CN){κ^4-(1*R*,2*R*)-PNNP}][BF_4] (**1**) and *cis*-[RuCl(CH_3CN){κ^4-(1*R*,2*R*)-P(NH)(NH)P}][BF_4] (**2**), respectively. When **1** was refluxed in pyridine (py), the coordinated CH_3CN was replaced by pyridine to form *cis*-[RuCl(py){κ^4-(1*R*,2*R*)-PNNP}][BF_4] (**3**). However, when **2** was refluxed in pyridine, one of the amino moieties (–CH_2–NH–)was oxidized to an imino moiety (–CH=N–) with concomitant displacement of the coordinated CH_3CN by pyridine to produce *cis*-[RuCl(py){κ^4-(1*R*,2*R*)-P(N)(NH)P}][BF_4] (**4**). The structures of **3** and **4** were ascertained by X-ray crystallography. Compounds **1**–**4** are effective catalysts for the epoxidation of various olefins with air. A turnover frequency of up to 733 h^{-1} and an enantiomeric excess of up to 24% were obtained for the epoxidation of styrene catalysed by **2**. Compound **2** can also catalyse the epoxidation, dehydrogenation and C–H activation of various olefins, alcohols and alkanes by *tert*-butyl hydroperoxide with high chemical selectivity.

Introduction

Diamino-, diimino- and diamidodiphosphanes are very versatile ligands. Their transition metal complexes are effective catalysts for asymmetric hydrogenation,[1] epoxidation,[2] cyclopropanation,[3] and allylic alkylation.[4,5] Thus, the synthesis of chiral diamino-, diimino- and diamidodiphosphane ligands and their applications as auxiliaries for the preparation of chiral catalysts have aroused considerable interest. We have investigated the preparation and chemistry of such phosphanes,[5−10] and reported the synthesis of (1*R*,2*R*)-*N*,*N*′-bis[2-(diphenylphosphanyl)benzylidene]-1,2-diiminocyclohexane [(1*R*,2*R*)-PNNP], (1*R*,2*R*)-*N*,*N*′-bis[2-(diphenylphosphanyl)benzylidene]-1,2-diaminocyclohexane [(1*R*,2*R*)-P(NH)(NH)P], and their Ru^{II},[8] Cu^{I} and Ag^{I} [9] complexes. Recently, we reported the synthesis, structure and catalytic activity of *trans*-[$RuCl_2${κ^3-(1*R*,2*R*)-P(NH)(NH)P}(PPh_3)][11] and its nonchiral analogue *trans*-[$RuCl_2${κ^3-P(NH)(NH)P}(PPh_3)] {P(NH)(NH)P = *N*,*N*′-bis[2-(diphenylphosphanyl)benzylidene]-1,2-diaminoethane}.[12] Here we describe the synthesis of *cis*-[RuCl(CH_3CN){κ^4-(1*R*,2*R*)-PNNP}][BF_4] (**1**), *cis*-[RuCl(CH_3CN)-{κ^4-(1*R*,2*R*)-P(NH)(NH)P}][BF_4] (**2**), *cis*-[RuCl(py){κ^4-(1*R*,2*R*)-PNNP}][BF_4] (**3**) and *cis*-[RuCl(py){κ^4-(1*R*,2*R*)-P(NH)NP}][BF_4] (**4**), and their applications in catalytic oxidation. The crystal structures of **3** and **4** are also presented.

[a] Department of Chemistry, Hong Kong Baptist University
Waterloo Road, Kowloon Tong, Hong Kong
Fax: (internat.) + 852/3411-5862
E-mail: wkwong@hkbu.edu.hk

Results and Discussion

Synthesis and Characterisation of the Complexes

Scheme 1 summarises the reactions leading to complexes **1**−**4**. One chloride ion from *trans*-[$RuCl_2${κ^4-(1*R*,2*R*)-PNNP}] or *trans*-[$RuCl_2${κ^4-(1*R*,2*R*)-P(NH)(NH)P}] was abstracted by $AgBF_4$ in CH_3CN at ambient temperature to afford the solvent-coordinated complex *cis*-[RuCl(CH_3CN){κ^4-(1*R*,2*R*)-PNNP}][BF_4] (**1**) or *cis*-[RuCl(CH_3CN){κ^4-(1*R*,2*R*)-P(NH)(NH)P}][BF_4] (**2**), respectively. The coordination of CH_3CN in **1** and **2** was revealed by their FAB MS, ^{1}H NMR and IR data. The $^{31}P\{^1H\}$ NMR spectra of both **1** and **2** exhibit two doublets [δ = 44.0 ($^2J_{P,P}$ = 24.3 Hz) and 49.8 ppm ($^2J_{P,P}$ = 24.3 Hz) for **1**; δ = 37.3 ($^2J_{P,P}$ = 24.5 Hz) and 44.1 ppm ($^2J_{P,P}$ = 24.5 Hz) for **2**], implying a *cis*-[RuCl(CH_3CN)] arrangement, which is further supported by the X-ray structures of the pyridine derivatives of **1** and **2** (vide infra).

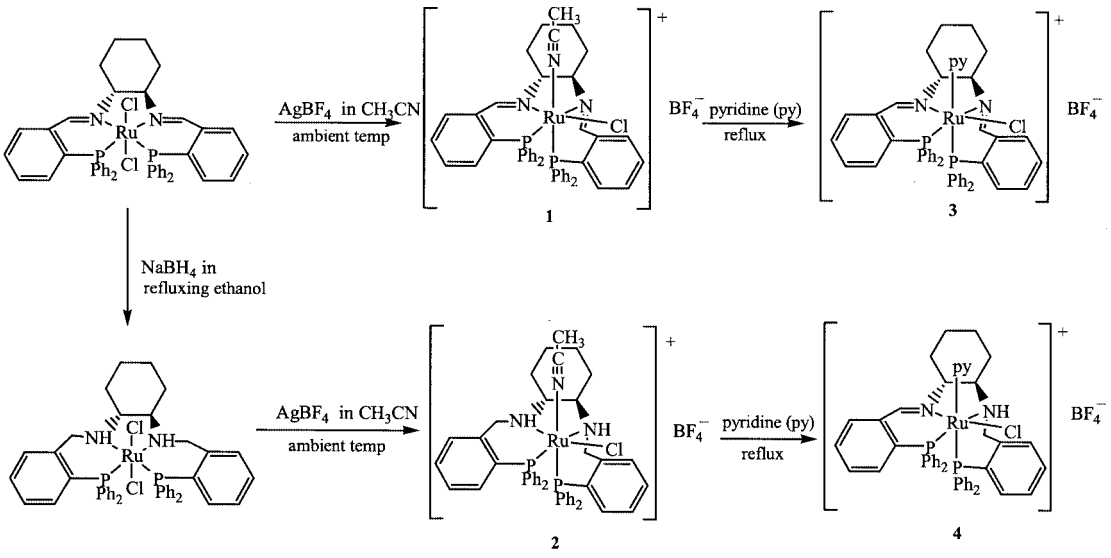

Scheme 1

When **1** was heated under reflux in pyridine the coordinated CH_3CN molecule was substituted by pyridine to give *cis*-[RuCl(py){κ⁴-(1*R*,2*R*)-PNNP}][BF_4] (**3**). The presence of the pyridine ligand was confirmed by FAB MS and ^1H NMR spectroscopic data. The $^{31}P\{^1H\}$ NMR spectrum of **3** exhibited two doublets at δ = 45.1 ($^2J_{P,P}$ = 29.5 Hz) and 46.7 ppm ($^2J_{P,P}$ = 29.5 Hz), suggesting two non-equivalent phosphorus atoms. The structure of **3** was ascertained by X-ray crystallography. A perspective drawing of the cation of **3** is shown in Figure 1. Selected bond lengths and angles are given in Table 1. The Ru atom adopts a distorted octahedral geometry with the chloro and pyridine ligands in a *cis* arrangement and the (1*R*,2*R*)-PNNP ligand behaving as a chelating tetradentate ligand. The chloro ligand is *trans* to the imino group N(1), whereas the pyridine group is

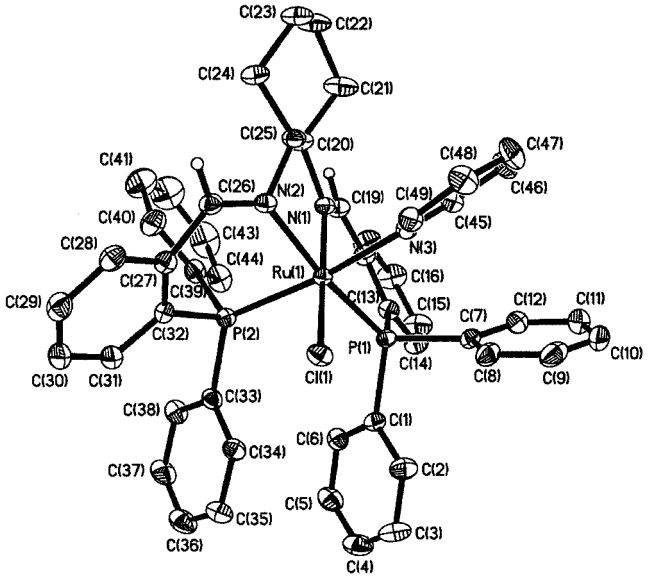

Figure 1. A perspective drawing of the cation of **3**, with the atoms shown at the 30% probability level; hydrogen atoms of the cyclohexyl, pyridine and phenyl rings are omitted for clarity

Table 1. Selected bond lengths [Å] and bond angles [°] for **3** and **4**

Complex **3**			
Ru(1)−N(1)	2.0436(19)	Ru(1)−N(2)	2.1251(17)
Ru(1)−N(3)	2.1799(17)	Ru(1)−P(1)	2.2946(5)
Ru(1)−P(2)	2.3104(5)	Ru(1)−Cl(1)	2.4326(6)
N(1)−C(19)	1.283(3)	N(2)−C(26)	1.260(3)
N(2)−C(25)	1.482(3)	N(1)−C(20)	1.528(3)
N(1)−Ru(1)−N(2)	78.58(7)	P(1)−Ru(1)−P(2)	100.00(2)
N(3)−Ru(1)−Cl(1)	88.18(5)	P(1)−Ru(1)−Cl(1)	94.16(2)
N(2)−Ru(1)−Cl(1)	94.38(6)	N(1)−Ru(1)−Cl(1)	171.54(5)
C(26)−N(2)−C(25)	118.67(17)	C(19)−N(1)−C(20)	113.50(19)
N(1)−Ru(1)−N(3)	86.63(7)	N(3)−Ru(1)−P(2)	168.17(5)
Complex **4**			
Ru(1)−N(1)	2.022(4)	Ru(1)−N(2)	2.162(3)
Ru(1)−N(3)	2.192(4)	Ru(1)−P(1)	2.2835(11)
Ru(1)−P(2)	2.3339(11)	Ru(1)−Cl(1)	2.4364(12)
N(1)−C(19)	1.296(6)	N(2)−C(31)	1.480(6)
N(1)−C(25)	1.527(5)	N(2)−C(30)	1.485(6)
N(1)−Ru(1)−N(2)	81.49(14)	N(1)−Ru(1)−N(3)	86.28(14)
N(2)−Ru(1)−N(3)	82.57(13)	N(1)−Ru(1)−P(1)	93.80(10)
N(1)−Ru(1)−Cl(1)	172.67(10)	N(3)−Ru(1)−Cl(1)	89.64(11)
P(1)−Ru(1)−Cl(1)	92.32(4)	P(1)−Ru(1)−P(2)	99.98(4)
N(1)−C(19)−C(12)	129.7(4)	N(2)−C(31)−C(32)	116.3(4)

trans to the diphenylphosphanyl group P(2). The Ru−P, Ru−Cl and Ru−N distances are in the ranges expected for similar (diamino- and diaminodiphosphane)ruthenium complexes.[1,8,11−13] The relatively short Ru(1)−N(1) bond [2.0436(19) Å] is a reflection of the *trans* influence. The difference between Ru(1)−N(2) [2.1251(17) Å] and Ru(1)−N(3) [2.1799(17) Å] may be attributed to the chelating effect of the tetradentate diiminodiphosphane ligand. The N(1)−C(19) [1.283(3) Å] and N(2)−C(26) [1.260(3) Å] distances fall in the normal range observed for carbon−nitrogen double bonds.[11,12]

When **2** was heated under reflux in pyridine one of the two amino moieties (−CH_2−NH−) of the tetradentate diaminodiphosphane ligand was oxidized to an imino moiety

(−CH=N−) with concomitant displacement of the coordinated CH_3CN by pyridine to give *cis*-[RuCl(py){κ⁴-(1*R*,2*R*)-P(NH)NP}][BF_4] (**4**), whose structure was established by X-ray crystallography. A perspective drawing of the cation of **4** is shown in Figure 2 and selected bond lengths and bond angles are listed in Table 1. Structural analysis revealed that the κ⁴-(1*R*,2*R*)-P(NH)(NH)P ligand had been oxidized to a κ⁴-(1*R*,2*R*)-P(NH)NP ligand with the amino group *trans* to the chloride ion oxidized to an imino group. The N(1)−C(19) and N(2)−C(31) distances [1.296(6) and 1.480(6) Å] lie in the normal ranges observed for carbon−nitrogen double and single bonds, respectively. The Ru atom adopts a slightly distorted octahedral geometry with a *cis* arrangement of the chloro and pyridine ligands. The Ru−P, Ru−Cl and Ru−N distances are similar to those of **3**. The Ru−P bond [Ru(1)−P(1) 2.2835(11) Å] *trans* to the amino group N(2) is shorter than that [Ru(1)−P(2) 2.3133(11) Å] *trans* to the pyridine group N(3) due to the *trans* influence. The difference in Ru−N distances [Ru−N(1) 2.022(4) Å vs. Ru(1)−N(2) 2.162(3) Å] implies that the imino nitrogen atom, N(1), is more tightly bound to the Ru centre than the amino nitrogen atom, N(2), presumably due to dπ−pπ back donation to the imino group. The N(1)−Ru(1)−Cl(1) angle of 172.67(10)° indicates that the chloro ligand is *trans* to the imino nitrogen atom. This configuration is favoured over the alternative with *trans*-Cl−Ru−N(amine) as an imino nitrogen atom is a better π-acceptor than an amino nitrogen atom. The solid-state structure of **4** is consistent with its $^{31}P\{^1H\}$ and ^1H NMR, IR and FAB MS data. The $^{31}P\{^1H\}$ NMR spectrum shows two doublets at δ = 42.7 ($^2J_{P,P}$ = 28.8 Hz) and 52.7 ppm ($^2J_{P,P}$ = 28.8 Hz), which can be assigned to P(1) and P(2), respectively (Figure 2). The presence of the imino group is further supported by the ^1H NMR spectrum, which shows a broad singlet at δ = 9.42 ppm for the −C*H*=N− proton. The IR spectrum also shows the *ν*(C=N) absorption at 1657 cm^{-1}. Oxidation of the coordinated amino moiety to a coordinated imino moiety has been reported recently for related (diaminodiphosphane)ruthenium complexes. At room temperature, *trans*-[$RuCl_2${κ³-(1*R*,2*R*)-P(NH)(NH)P}(PPh_3)] was slowly oxidized by air to *trans*-[$RuCl_2${κ³-(1*R*,2*R*)-P(NH)NP}(PPh_3)],[11] and *trans*-[$RuCl_2${κ³-P(NH)(NH)P(O)}(PPh_3)] by H_2O_2 to *trans*-[$RuCl_2${κ³-P(NH)NP(O)}(PPh_3)].[12] In both cases one of the two coordinated amino moieties was oxidized to a coordinated imino moiety.

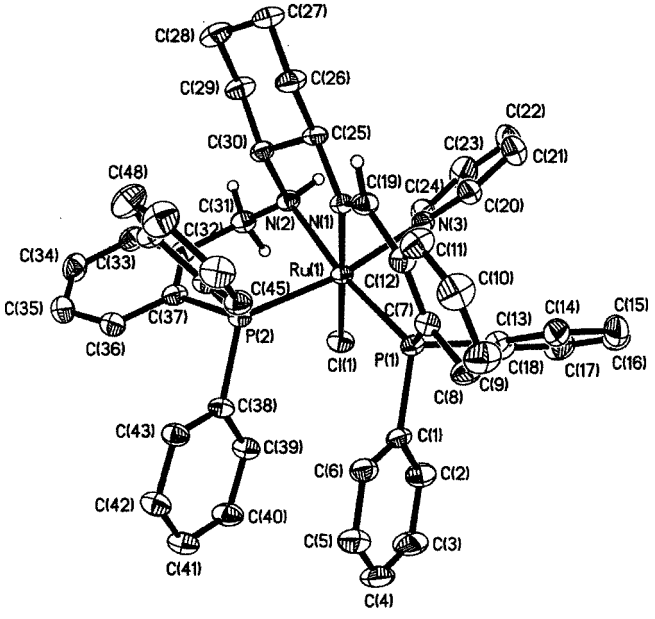

Figure 2. A perspective drawing of the cation of **4**, with the atoms shown at the 30% probability level; hydrogen atoms of the cyclohexyl, pyridine and phenyl rings are omitted for clarity

Catalytic Oxidation

Ruthenium-catalysed oxidation of alkenes with various oxidants has drawn considerable interest recently, but there are very few studies on aerobic oxidation.[11,12,14,15] In this work, air was chosen as one of the oxidants. Furthermore, complexes **1**−**4** were employed as the catalysts for the asymmetric oxidation of olefins. Styrene, the first substrate we used, gave three main products, namely styrene oxide, benzaldehyde and phenylacetaldehyde (Table 2). Nevertheless, with **4** as the catalyst, styrene was converted into styrene oxide with exceptionally high selectivity (80%). Presumably, epoxidation prevails over the oxidative cleavage of the C=C double bond. In addition, the enantioselectivity of all these catalytic epoxidation reactions is comparatively low. However, the highest TOF (733 h^{-1}) and the highest enantiomeric excess (*ee*) (24%) were obtained with **2**. Therefore, complex **2** was chosen to study the catalytic asymmetric oxidation of various olefins with air (Table 3). Although conversions of sterically crowded *cis*- and *trans*-stilbene were expected, and found, to be very low, those of α-methylstyrene and 1,2-dihydronaphthalene were as good as that of styrene. It is noteworthy that the catalytic oxidation of α-methylstyrene and 1,2-dihydronaphthalene with air using **2** selectively gave acetophenone and 1,2-dihydronaphthalene epoxide, respectively. Unfortunately, only a moderate *ee* was obtained from α-methylstyrene, which is attributed to the formation of a planar intermediate. In addition, the dependence of the asymmetric oxidation of styrene using **2** on various oxidants was investigated (Table 4). *tert*-Butyl hydroperoxide (TBHP) clearly gave the highest TOF and the highest selectivity for styrene oxide but only with poor enantioselectivity. The catalytic oxidation probably proceeds via a planar species, without the involvement of a chiral metal centre as an active intermediate. Investigation on the mechanism of the autoxidation of olefins is in progress.

The catalytic activity of **2** towards the oxidation of organic substrates with TBHP has also been studied (Table 5). In control experiments, no oxidized product was detected in the absence of either **2** or TBHP. Complex **2** catalysed the oxidation of styrene (Entry 1), with TBHP giving styrene oxide as the major product along with benzylaldehyde, possibly by C=C cleavage, and phenylacetaldehyde; α-methylstyrene (Entry 2) mainly afforded phenylacetalde-

Table 2. Asymmetric oxidation of styrene with air using **1**−**4** as catalysts

Catalyst	TOF [h^{-1}][a]	Selectivity (%)[b] Styrene oxide (*ee* in %)[c]	Benzaldehyde	Phenylacetaldehyde
1	704	47 (11)	44	9
2	733	43 (24)	53	3
3	451	33 (23)	43	16
4	352	80 (18)	18	2

[a] Determined by GC analysis based on the starting substrate using an internal standard. [b] Identified by GC-MS. [c] Determined by GC analysis with a chiral column based on an internal standard.

Table 3. Asymmetric oxidation of olefins with air using **2** as catalyst

Substrate	Conv. (%)[a]	Selectivity (%)[b] Epoxide (*ee* in %) [c]	Benzaldehyde
Styrene	52	43 (24)	53
α-Methylstyrene	32	7.5 (23.4)	89[d]
1,2-Dihydronaphthalene	64	96 (0)	0
cis-Stilbene	9	53 (0)	19
trans-Stilbene	2	28 (0)	39

[a] Determined by GC analysis based on the starting substrate using an internal standard. [b] Identified by GC-MS. [c] Determined by GC analysis with a chiral column based on an internal standard. [d] Acetophenone was obtained.

Table 4. Asymmetric oxidation of styrene with various oxidants using **2** as catalyst

Oxidant	TOF [h^{-1}][a]	Selectivity (%)[b] Styrene oxide (*ee* in %) [c]	Benzaldehyde	Phenylacetaldehyde
TBHP	305	53 (2.3)	31	12
H_2O_2	55	11 (7.8)	84	5.5
$NaIO_4$	61	45 (23.7)	37	15
NaOCl	38	0 (0)	87	13

[a] Determined by GC analysis based on the starting substrate using an internal standard. [b] Identified by GC-MS. [c] Determined by GC analysis with a chiral column based on an internal standard.

hyde. Notably, *cis*- and *trans*-stilbene (Entries 3 and 4) were selectively oxidized to 2,3-diphenyloxirane whereas oxidation of 1,2-dihydronaphthalene (Entry 5) gave only naphthalene; we believe that the formation of a highly conjugated system provides the necessary driving force for the conversion. It is interesting that the oxidation of *cis*-cyclooctene (Entry 6) and of norbornene (Entry 7) produced predominantly 9-oxabicyclo[6.1.0]nonane and 2,3-epoxynorbornane, respectively, whereas oxidation of cyclohexene (Entry 8) afforded 2-cyclohexen-1-one as the major product. The oxidation of cyclohexene (Entry 9) was notably suppressed when 2,6-di-*tert*-butyl-4-methylphenol was added to the reaction mixture, which suggests a substantial radical character in the active intermediate.[16] When the terminal oxidant was changed from TBHP to cumene hydroperoxide (CHP), the product profile (Entry 10) is dominated by cumene, acetophenone and 2-phenyl-2-propanol, which are presumably generated by β-scission of cumyloxy radicals. The oxidation of cyclohexene by TBHP might involve abstraction of the allylic hydrogen atom from the relatively flexible six-membered ring to give an allylic free radical intermediate that can be stabilized by the π-system of the double bond; this is unlikely to occur with *cis*-cyclooctene and norbornene due to inefficient allylic stabilisation in the more rigid and nonplanar norbornenyl and cyclooctenyl radicals. Conversely, the epoxidation of norbornene and *cis*-cyclooctene could result from the homolytic addition of the *t*BuOO$^{\cdot}$ species to the more strained double bond, followed by homolytic cyclisation.[17−20] The homolytic mechanism accords with the absence of epoxidation with cyclohexene, which is less prone to addition of peroxy radicals. Indeed, the predominance of peroxy substitution follows from the ease with which H-atom abstraction occurs from the allylic position of cyclohexene.

Moreover, complex **2** would also be an efficient catalyst for the oxidation of alcohol with TBHP. In the presence of 2 equiv. of TBHP in benzene, complex **2** catalysed the oxidation of primary alcohols (Entries 11 and 12, Table 5) to the corresponding acid and/or ester, of secondary alcohols (Entries 13 and 14) to the corresponding ketones, and of phenol (Entries 15 and 16) to *p*-benzoquinone. Minisci and co-workers have reported (porphyrin)Fe^{III}-catalysed oxidation of phenol to *p*-benzoquinone by TBHP by a free

Table 5. Catalytic oxidation of organic compounds with TBHP using **2** as catalyst

Entry	Substrate	Conv. (%)[a]	Product[b]	Selectivity (%)[c]
1	styrene	86	benzylaldehyde	31
			styrene oxide	53
			phenylacetaldehyde	12
2	α-methylstyrene	88	phenylacetaldehyde	96
3	*trans*-stilbene	70	benzaldehyde	15
			benzoic acid	17
			2,3-diphenyloxirane	58
4	*cis*-stilbene	15	benzaldehyde	19
			benzoic acid	3.5
			2,3-diphenyloxirane	71
5	1,2-dihydronaphthalene	85	naphthalene	97
6	*cis*-cyclooctene	39	9-oxabicyclo[6.1.0]nonane	95
7	norbornene	27	2,3-epoxynorbornane	96
8	cyclohexene	17	2-cyclohexen-1-ol	2
			2-cyclohexen-1-one	95
9	cyclohexene[d]	1.1	2-cyclohexen-1-one	96
10	cyclohexene[e]	1.1	2-cyclohexen-1-ol	1
			2-cyclohexen-1-one	1
			cumene	11
			acetophenone	29
			2-phenyl-2-propanol	29
11	benzyl alcohol	75	benzoic acid	75
			benzyl benzoate	20
12	3-methyl-1-butanol	58	3-methylbutyl 3-methylbutanoate	94
13	2-nonanol	77	2-nonanone	99
14	cyclohexanol	59	cyclohexanone	98
15	phenol	49	*p*-benzoquinone	95
16	phenol[f]	80	*p*-benzoquinone	96
17	*n*-octane	4	2-octanone	33
			4-octanone	61
18	cyclohexane	1	cyclohexanol	22
			cyclohexanone	77
19	cyclohexane[g]	1	cyclohexanol	37
			cyclohexanone	39
			cyclohexyl chloride	18
20	cyclohexane[h]	2	cyclohexanol	1
			cyclohexanone	1.1
			cumene	9
			acetophenone	27
			2-phenyl-2-propanol	29
21	adamantane	30	adamantan-1-ol	59
			2-adamantanone	35
22	*n*-propylbenzene	17	1-phenyl-1-propanone	98
23	ethylbenzene	36	acetophenone	96
24	diphenylmethane	73	benzophenone	99
25	cumene	40	2-phenyl-2-propanol	85
			acetophenone	8
26	1,3-diisopropylbenzene	58	2,4-diisopropylphenol	94

[a] Determined by GC analysis based on the starting substrate using an internal standard. [b] Identified by GC-MS. [c] Selectivity: determined by GC analysis based on the amount of converted substrate using an internal standard. [d] 2,6-Di-*tert*-butyl-4-methylphenol (0.35 g, 1.60 mmol) was also added to the reaction mixture. [e] Cumene hydroperoxide was used as the oxidant. [f] Triethylamine (0.09 mmol) was also added to the reaction mixture. [g] Benzene/CCl_4 (9:1, v/v) as solvent. [h] Cumene hydroperoxide was used as the oxidant.

radical mechanism.[21] They found that addition of a nitrogen-containing base such as pyridine enhanced the production of *p*-benzoquinone by catalyzing the decomposition of the alkylperoxy intermediate. We used a similar strategy to test the involvement of reactive free radical species during catalysis and found that the rate of *p*-benzoquinone formation was enhanced by the addition of triethylamine, which is consistent with the formation of a *tert*-butylperoxy intermediate.[21]

Furthermore, complex **2** can catalyse the oxidation of unactivated saturated C−H bonds with TBHP. Alkanes (Table 5, Entries 17, 18 and 21) were oxidized to their corresponding ketones, alcohols or a mixture of both. In the presence of 2 equiv. of TBHP and a catalytic amount of **2**, *n*-octane was oxidized to a mixture of 2-octanone and 4-octanone, cyclohexane to a mixture of cyclohexanol and cyclohexanone, and adamantane to adamantan-1-ol and 2-adamantone. The results revealed that oxidation of *n*-

octane proceeded by secondary C−H bond activation exclusively with no detectable products from primary C−H bond activation, and that adamantane preferentially gave a tertiary alcohol. Presumably, alkane oxidation proceeded by an H-atom abstraction pathway to give a relatively stable free radical intermediate. This is supported by the formation of cyclohexyl chloride (Entry 19) along with cyclohexanone and cyclohexanol upon catalytic oxidation of cyclohexane by TBHP in the presence of CCl_4. Moreover, copious formation of cumene, acetophenone and 2-phenyl-2-propanol (Entry 20) from cumene hydroperoxide also implies an alkylperoxy radical as the transient intermediate.[22] A similar mechanism has been proposed for the ruthenium-catalysed oxidation of alkanes with TBHP.[23] Under similar conditions, *n*-propylbenzene (Entry 22) was oxidized to 1-phenyl-1-propanone, ethylbenzene (Entry 23) to acetophenone, diphenylmethane (Entry 24) to benzophenone, cumene (Entry 25) to a mixture of 2-phenyl-2-propanol and acetophenone, and 1,3-diisopropylbenzene (Entry 26) to 2,4-diisopropylphenol. It is obvious that the activity of arylalkanes towards oxidation by **2** is higher than those of nonarylalkanes and it is consistent with the relative stability of the radicals generated by H-atom abstraction, i.e. aryl-substituted radicals are more stable than unsubstituted radicals. Experimental evidence suggests that free radicals are probably involved in the catalytic oxidation of various organic substrates. In general, the oxidation of a series of organic substrates with TBHP by complex **2** involves a free radical mechanism.

Conclusion

We have described the synthesis, characterisation and structural studies of a series of new chiral cationic (diimino- and diaminodiphosphane)ruthenium complexes. Detailed investigations of their catalytic properties in the asymmetric oxidations of various organic molecules show that these chiral complexes effectively catalyse the epoxidation of a range of alkenes with air; the data are compared to those using other oxidants. Experimental evidence suggests that free radicals are probably involved in the catalytic oxidation processes associated with these chiral complexes.

Experimental Section

General Remarks: Unless otherwise stated, all experiments were conducted under dry nitrogen. Solvents were dried by standard procedures, distilled and deaerated before use. Reagent grade chemicals were used and, where appropriate, degassed before use. All organic substrates were purified by literature methods, and their purities verified by GC or ^{1}H NMR analysis. Melting points were taken in sealed capillaries and are uncorrected. The compounds *trans*-[$RuCl_2${κ^4-(1*R*,2*R*)-PNNP}][8] and *trans*-[$RuCl_2${κ^4-(1*R*,2*R*)-P(NH)(NH)P}][11] were prepared according to literature methods. IR spectra (KBr pellets) were recorded with a Nicolet Nagna-IR 550 spectrometer and NMR spectra with a JEOL EX270 spectrometer. Chemical shifts of ^{1}H NMR spectra were referenced to internal deuterated solvents and then recalculated to TMS (δ = 0.00 ppm) and those of ^{31}P{^{1}H} NMR spectra were referenced to external 85% H_3PO_4. Low-resolution mass spectra were obtained with Finnigan MAT SSQ-710 and MAT 95 spectrometers in positive FAB mode and are reported as *m*/*z*. Gas chromatograms were obtained with an HP 5890 GC system equipped with an FID detector or an HP 6890−5972 GC-MSD system. An HP 5890 GC equipped with a WCOT fused silica capillary column (25 × 0.25 mm, 0.25-μm film, Varian) was used for chiral analyses. Microanalyses were performed by the Shanghai Institute of Organic Chemistry, Chinese Academy of Sciences. The progress of all reactions was monitored by ^{31}P{^{1}H} NMR spectroscopy.

***cis*-[RuCl(CH_3CN){κ^4-(1*R*,2*R*)-PNNP}][BF_4] (1):** A red solution of *trans*-[$RuCl_2${κ^4-(1*R*,2*R*)-PNNP}] (0.260 g, 0.313 mmol) in acetonitrile (10 mL) was added dropwise to a solution of $AgBF_4$ (0.062 g, 0.318 mmol) in acetonitrile (10 mL). The mixture was then stirred at ambient temperature for 24 h to give an orange solution with a white precipitate. The solution was filtered and the solvents evaporated to dryness. The resultant orange residue was redissolved in CH_2Cl_2 and filtered. Diethyl ether was added and the mixture was then cooled to 0 °C to give an orange solid that was filtered off, washed with diethyl ether and *n*-hexane, and dried in vacuo. Yield: 0.220 g, 76%; m.p. 180−182 °C (dec). IR (KBr): $\tilde{\nu}$ = 3059 s, 2932 m, 2858 m, 1964 m, 1642 s, 1434 s, 1085 br, 749 s, 702 s, 527 s cm^{-1}. ^{1}H NMR ($CDCl_3$): δ = 1.20−2.31 (m, 8 H, CH_2CH_2), 2.53 (s, 3 H, CH_3CN), 3.71 (m, 2 H, NC*H*−C*H*N), 6.37−7.76 (m, 28 H, aryl *H*), 8.77 (d, $^3J_{P-H}$ = 10.0 Hz, 1 H, −C*H*=N−), 8.97 (d, $^3J_{P-H}$ = 8.6 Hz, 1 H, −C*H*=N−) ppm. ^{31}P{^{1}H} NMR ($CDCl_3$): δ = 44.0 (d, $^2J_{P,P}$ = 24.3 Hz), 49.8 (d, $^2J_{P,P}$ = 24.3 Hz) ppm. FAB MS: *m*/*z* = 836 [M − BF_4]$^+$, 795 [M − CH_3CN − BF_4]$^+$. $C_{46}H_{43}BClF_4N_3P_2Ru\cdot1.5CH_2Cl_2\cdot H_2O$ (1068.56): calcd. C 53.38, H 4.54, N 3.93; found C 53.01; H 4.62; N 4.11. $[\alpha]_D^{20}$ = −91.56 (*c* = 0.5, CH_2Cl_2).

***cis*-[RuCl(CH_3CN){κ^4-(1*R*,2*R*)-P(NH)(NH)P}][BF_4] (2):** *trans*-[$RuCl_2${κ^4-(1*R*,2*R*)-P(NH)(NH)P}] (0.400 g, 0.480 mmol) and $AgBF_4$ (0.100 g, 0.513 mmol) were dissolved in acetonitrile (40 mL) and the mixture stirred at ambient temperature for 24 h. A yellow solution with a white precipitate was obtained. The solution was filtered and the solvents evaporated to dryness in vacuo. The resultant yellow residue was then redissolved in CH_2Cl_2 and *n*-hexane was added to initiate the crystallisation of the product as a yellow solid. Yield: 0.400 g, 90%; m.p. 189−190 °C (dec). IR (KBr): $\tilde{\nu}$ = 3431 s, 3053 m, 2934 m, 1963 m, 1476 m, 1439 s, 1077 vs, 746 s, 700 s, 519 s cm^{-1}. ^{1}H NMR ($CDCl_3$): δ = 1.58−2.04 (m, 8 H, CH_2CH_2), 2.62 (s, 3 H, CH_3CN), 2.81−3.01 (m, 4 H, CH_2N), 3.65 (m, 2 H, NC*H*−C*H*N), 4.21 (m, 2 H, N*H*), 6.71−8.00 (m, 28 H, aryl *H*) ppm. ^{31}P{^{1}H} NMR ($CDCl_3$): δ = 37.3 (d, $^2J_{P,P}$ = 24.5 Hz), 44.1 (d, $^2J_{P,P}$ = 24.5 Hz) ppm. FAB MS: *m*/*z* = 840 [M − BF_4]$^+$, 799 [M − CH_3CN − BF_4]$^+$. $C_{46}H_{47}BClF_4N_3P_2Ru\cdot CH_2Cl_2\cdot 2H_2O$ (1048.14): calcd. C 53.81, H 5.06, N 4.01; found C 53.71, H 5.16, N 3.92. $[\alpha]_D^{20}$ = 72.80 (*c* = 0.5, CH_2Cl_2).

***cis*-[RuCl(py){κ^4-(1*R*,2*R*)-PNNP}][BF_4] (3):** Complex **1** (0.100 g, 0.108 mmol) was dissolved in pyridine (20 mL) and the mixture was heated under reflux for 30 min in air and then all volatile components were removed in vacuo. The resultant residue was washed with diethyl ether and recrystallised from CH_2Cl_2/*n*-hexane to give red crystals. Yield: 0.085 g, 82%; m.p. 197−198 °C (dec). IR (KBr): $\tilde{\nu}$ = 3058 m, 2924 m, 1636 m, 1486 m, 1439 s, 1310 m, 1088 vs, 752 m, 700 m, 524 s cm^{-1}. ^{1}H NMR ($CDCl_3$): δ = 0.90−1.82 (m, 8 H, CH_2CH_2), 2.49 (m, 1 H, NCH−C*H*N), 2.78 (m, 1 H, NC*H*−CHN), 6.58−7.90 (m, 28 H, aryl *H*), 8.30 (d, $^3J_{P-H}$ = 8.7 Hz, 1 H, −C*H*=N−), 8.41 (m, 3 H, pyridyl *H*s), 8.72 (d,

$^3J_{P-H}$ = 8.7 Hz, 1 H, −C*H*=N−), 9.03 (m, 2 H, pyridyl *H*) ppm. $^{31}P\{^1H\}$ NMR ($CDCl_3$): δ = 45.1 (d, $^2J_{P,P}$ = 29.5 Hz), 46.7 (d, $^2J_{P,P}$ = 29.5 Hz) ppm. FAB MS: *m*/*z* = 874 $[M - BF_4]^+$, 795 $[M - py - BF_4]^+$. $C_{49}H_{45}BClF_4N_3P_2Ru{\cdot}CH_2Cl_2{\cdot}2H_2O$ (1082.15): calcd. C 55.49, H 4.76, N 3.88; found C 55.73, H 4.95, N 3.87. $[\alpha]_D^{20}$ = −45.85 (*c* = 0.5, CH_2Cl_2).

***cis*-[RuCl(py){κ⁴-(1*R*,2*R*)-P(NH)NP}][BF₄] (4):** Complex **2** (0.100 g, 0.108 mmol) was added to pyridine (20 mL) and the mixture heated under reflux for 6 h in air. All volatiles were then removed in vacuo and the residue was washed, with *n*-hexane and toluene, and then recrystallised from CH_2Cl_2/toluene to give an orange solid. Yield: 0.070 g, 67%; m.p. 185−186 °C. IR (KBr): ν̃ = 3058 m, 2955 m, 1657 m, 1558 m, 1481 m, 1429 s, 1258 s, 1083 vs, 803 s, 746 m, 695 s, 524 s cm^{-1}. ^1H NMR ($CDCl_3$): δ = 1.69−2.01 (m, 8 H, C*H*$_2$C*H*$_2$), 2.51 (m, 1 H, CH*H*N), 2.76 (m, 1 H, C*H*HN), 3.67 (m, 1 H, −NCH−C*H*N−), 4.45 (m, 2 H, N*H* and −NC*H*−CHN−), 6.24−8.59 (m, 33 H, aryl and pyridyl *H*), 9.42 (br. s, 1 H, −C*H*=N−) ppm. $^{31}P\{^1H\}$ NMR ($CDCl_3$): δ = 42.69 (d, $^2J_{P,P}$ = 28.8 Hz), 52.71 (d, $^2J_{P,P}$ = 28.8 Hz) ppm. FAB MS: *m*/*z* = 876 $[M - BF_4]^+$, 797 $[M - py - BF_4]^+$. $C_{49}H_{47}BClF_4N_3P_2Ru{\cdot}C_7H_8$ (1055.35): calcd. C 63.72, H 5.26, N 3.98; found C 63.58, H 5.37, N 3.90. $[\alpha]_D^{20}$ = 81.31 (*c* = 0.5, CH_2Cl_2).

General Procedure for Catalytic Oxidation by Air: A reaction mixture of organic substrate (3.0 g) and catalyst (0.001 mmol) was stirred in open air at 80 °C for 16 h. The resultant solution was analysed by GC, and the identity of the analytes verified by GC-MS and standard compounds (Tables 2 and 3). Control experiments were performed in the absence of catalyst under identical conditions.

General Procedure for Catalytic Oxidation by TBHP: A solution of organic substrate (1.5 mmol), TBHP (80% in di-*tert*-butyl peroxide, 3.2 mmol) and **2** (1.0 mg, 0.001 mmol) in benzene (3 mL) was stirred under nitrogen at ambient temperature for 16 h. The reaction mixture was then poured slowly into a 10% aqueous Na_2SO_3 solution (5 mL) to destroy any remaining TBHP and the resultant solution was extracted with dichloromethane (2 × 5 mL). The organic layer was separated, dried with anhydrous Na_2SO_4 and analysed by GC (Tables 4 and 5). The identity of the analytes was verified by GC-MS and standard compounds. Control experiments without either the catalyst or TBHP were performed under identical conditions.

General Procedure for Catalytic Oxidation by H_2O_2: Styrene (0.16 g, 1.5 mmol) and **2** (2.0 mg, 0.002 mmol) were dissolved in acetone (3 mL). Aqueous hydrogen peroxide [0.29 g, 35% (w/w), 3.0 mmol] was then added as one portion and the reaction mixture was stirred under nitrogen at ambient temperature for 16 h, and then slowly poured into a 10% aqueous Na_2SO_3 solution (5 mL) to destroy any remaining H_2O_2. The resultant solution was extracted with dichloromethane (2 × 5 mL) and the organic layer was separated, dried with anhydrous Na_2SO_4 and analysed by GC (Table 4). Control experiments without either the catalyst or H_2O_2 were performed under identical conditions.

General Procedure for Catalytic Oxidation by $NaIO_4$: Styrene (0.16 g, 1.5 mmol) and **2** (2.0 mg, 0.002 mmol) were dissolved in acetone (3 mL). $NaIO_4$ (0.64 g, 3.0 mmol) was then added as one portion and the reaction mixture was stirred under nitrogen at ambient temperature for 16 h. The resultant solution was analysed by GC (Table 4). Control experiments in the absence of either the catalyst or $NaIO_4$ were performed under identical conditions.

General Procedure for Catalytic Oxidation by NaOCl: Styrene (0.16 g, 1.5 mmol) and **2** (2.0 mg, 0.002 mmol) were dissolved in acetone (3 mL). An excess of aqueous NaOCl was added as one portion and the reaction mixture was stirred under nitrogen at ambient temperature for 16 h. The resultant solution was analysed by GC (Table 4). Control experiments in the absence of either the catalyst or NaOCl were performed under identical conditions.

X-ray Crystallographic Studies: Pertinent crystallographic data and other experimental details are summarised in Table 6. Crystals of **3**·1.5CH_2Cl_2 and **4**·1.5CH_2Cl_2 suitable for X-ray diffraction studies

Table 6. Crystallographic data for complexes **3** and **4**

	3·1.5CH_2Cl_2	**4**·1.5CH_2Cl_2
Empirical formula	$C_{49}H_{45}BClF_4N_3P_2Ru{\cdot}1.5CH_2Cl_2$	$C_{49}H_{47}BClF_4N_3P_2Ru{\cdot}1.5CH_2Cl_2$
Formula mass	1088.53	1090.55
Crystal size [mm]	0.20 × 0.15 × 0.10	0.20 × 0.15 × 0.12
Crystal system	monoclinic	monoclinic
Space group	*C*2	*C*2
a [Å]	35.122(2)	35.0430(19)
b [Å]	10.4480(7)	10.4501(6)
c [Å]	13.0196(8)	13.4397(7)
α [°]	90	90
β [°]	91.143(2)	93.8820(10)
γ [°]	90	90
V [Å^3]	4776.7(5)	4910.4(5)
Z	4	4
T [K]	293	293
μ(Mo-K_α) [mm^{-1}]	0.674	0.656
F(000)	2208	2216
θ range [°]	1.93−27.51	1.52−27.51
Reflections collected	14010	14609
Independent reflections (R_{int})	8351 (0.0168)	7466 (0.0272)
Observed reflections	7267	6535
Goodness-of-fit on F^2	1.060	1.029
*R*1, *wR*2 [$I > 2\sigma(I)$]	0.0348, 0.0987	0.0358, 0.0896
*R*1, *wR*2 (all data)	0.0361, 0.0999	0.0440, 0.0981

were grown by slow concentration of solutions of **3** and **4** in CH_2Cl_2/*n*-hexane. The crystals were wrapped in epoxy glue, to prevent solvent loss, and mounted on a thin glass fibre. No decay in intensity was encountered during the data collection. Intensity data were collected at 293 K with a Bruker Axs SMART 1000 CCD area-detector diffractometer using graphite-monochromated Mo-K_α radiation. The collected frames were processed with the software SAINT[24] and an absorption correction was applied (SADABS)[25] to the collected reflections. The structures were solved by direct methods (SHELXTL™)[26] and refined against F^2 by full-matrix least-squares analysis. All non-hydrogen atoms were refined anisotropically. Except for the hydrogen atoms of the solvent molecules in **3** and **4**, which were not located, all other hydrogen atoms were generated in their idealised positions and allowed to ride on their respective parent carbon atoms. CCDC-204329 and -204330 contain the supplementary crystallographic data for this paper. These data can be obtained free of charge at www.ccdc.cam.ac.uk/conts/retrieving.html [or from the Cambridge Crystallographic Data Centre, 12 Union Road, Cambridge CB2 1EZ, UK; Fax: (internat.) + 44-1223/336-033; E-mail: deposit@ccdc.cam.ac.uk].

Acknowledgments

W. K. W. thanks the Hong Kong Baptist University and the Hong Kong Research Grants Council (HKBU 2053/97P) for financial support.

[1] J. X. Gao, T. Ikariya, R. Noyori, *Organometallics* **1996**, *15*, 1087−1089.
[2] R. M. Stoop, A. Mezzetti, *Green Chem.* **1999**, *1*, 39−41.
[3] B. M. Trost, *Acc. Chem. Res.* **1996**, *29*, 355−364.
[4] C. P Butts, J. Crosby, G. C. Lloyd-Jones, S. C. Stephen, *Chem. Commun.* **1999**, 1707−1708.
[5] J. H. Song, D. J. Cho, S. J. Jeon, Y. H. Kim, T. J. Kim, J. H. Jeong, *Inorg. Chem.* **1999**, *38*, 893−896.
[6] W. K. Wong, J. X. Gao, Z. Y. Zhou, T. C. W. Mak, *Polyhedron* **1993**, *12*, 1415−1417.
[7] J. X. Gao, H. L. Wan, W. K. Wong, M. C. Tse, W. T. Wong, *Polyhedron* **1996**, *15*, 1241−1251.
[8] W. K. Wong, T. W. Chik, X. Feng, T. C. W. Mak, *Polyhedron* **1996**, *15*, 3905−3907.
[9] W. K. Wong, T. W. Chik, K. N. Hui, I. Williams, X. Feng, T. C. W. Mak, C. M. Che, *Polyhedron* **1996**, *15*, 4447−4460.
[10] W. K. Wong, J. X. Gao, W. T. Wong, C. M. Che, *Polydedron* **1993**, *12*, 2063−2066.
[11] W. K. Wong, X. P. Chen, W. X. Pan, J. P. Guo, W. Y. Wong, *Eur. J. Inorg. Chem.* **2002**, 231−237.
[12] W. K. Wong, X. P. Chen, J. P. Guo, Y. G. Chi, W. X. Pan, W. Y. Wong, *J. Chem. Soc., Dalton Trans.* **2002**, 1139−1146.
[13] R. M. Stoops, S. Bachmann, M. Valentini, A. Mezzetti, *Organometallics* **2000**, *19*, 4117−4126.
[14] A. S. Goldstein, R. H. Beer, R. S. Drago, *J. Am. Chem. Soc.* **1994**, *116*, 2424−2429.
[15] C. A. Bessel, R. A. Leising, K. J. Takeuchi, *J. Chem. Soc., Chem. Commun.* **1991**, 833−835.
[16] T. Kojima, H. Matsuo, Y. Matsuda, *Inorg. Chim. Acta* **2000**, *300*, 661−667.
[17] J. Koola, D. Kochi, K. Jay, *J. Org. Chem.* **1987**, *52*, 4545−4553.
[18] D. E. V. Sickle, F. R. Mayo, R. M. Arluck, *J. Am. Chem. Soc.* **1965**, *87*, 4824−4832.
[19] A. Bottcher, M. W. Grinstaff, J. A. Labinger, H. B. Gray, *J. Mol. Catal. A: Chem.* **1996**, *113*, 191−200.
[20] K. Sato, M. Aoki, M. Ogawa, T. Hashimoto, D. Panyella, R. Noyori, *Bull. Chem. Soc. Jpn.* **1997**, *70*, 905−915.
[21] A. Brovo, F. Fontana, F. Minisci, *Chem. Lett.* **1996**, 401−402.
[22] D. W. Snelgrove, P. A. Macfaul, K. U. Ingold, M. D. D. Wayner, *Tetrahedron Lett.* **1996**, *37*, 823−826.
[23] C. M. Che, K. W. Cheng, M. C. W. Chan, T. C. Lau, C. K. Mak, *J. Org. Chem.* **2000**, *65*, 7996−8000.
[24] *SAINT, Reference manual*, Siemens Energy and Automation, Madison, WI, **1994−1996**.
[25] G. M. Sheldrick, *SADABS, Empirical Absorption Correction Program*, University of Göttingen, Germany, **1997**.
[26] G. M. Sheldrick, *SHELXTL™ Reference manual*, version 5.1, Siemens, Madison, WI, **1997**.

Received April 25, 2003

